



## Organometallic complexes for nonlinear optics. 52. Syntheses, structural, spectroscopic, quadratic nonlinear optical, and theoretical studies of $\text{Ru}(\text{C}_2\text{C}_6\text{H}_4\text{R}-4)(\kappa^2\text{-dppf})(\eta^5\text{-C}_5\text{H}_5)$ ( $\text{R} = \text{H}, \text{NO}_2$ )

Bandar A. Babgi<sup>a,b</sup>, Ahmed Al-Hindawi<sup>a</sup>, Graeme J. Moxey<sup>a</sup>, Fazira I. Abdul Razak<sup>a</sup>, Marie P. Cifuentes<sup>a</sup>, Erandi Kulasekera<sup>a</sup>, Robert Stranger<sup>a</sup>, Ayele Teshome<sup>c</sup>, Inge Asselberghs<sup>c</sup>, Koen Clays<sup>c</sup>, Mark G. Humphrey<sup>a,\*</sup>

<sup>a</sup> Research School of Chemistry, Australian National University, Canberra, ACT 0200, Australia

<sup>b</sup> Department of Chemistry, Faculty of Science, King Abdulaziz University, Jeddah 21589, Saudi Arabia

<sup>c</sup> Laboratory of Chemical and Biological Dynamics, Centre for Research on Molecular Electronics and Photonics, Katholieke Universiteit Leuven, Celestijnenlaan 200D, B-3001 Leuven, Belgium

### ARTICLE INFO

#### Article history:

Received 30 September 2012

Received in revised form

30 December 2012

Accepted 31 December 2012

Dedicated to the memory of Professor Gordon Stone, an inspirational organometallic chemist.

#### Keywords:

Crystal structure

Ruthenium

Alkynyl

Nonlinear optics

Density functional theory calculations

### ABSTRACT

The synthesis of  $\text{Ru}(\text{C}\equiv\text{CC}_6\text{H}_4-4\text{-NO}_2)(\kappa^2\text{-dppf})(\eta^5\text{-C}_5\text{H}_5)$  (**1**) is reported, together with spectroscopic, X-ray structural, linear optical and quadratic nonlinear optical (NLO) studies of **1** and  $\text{Ru}(\text{C}\equiv\text{CPh})(\kappa^2\text{-dppf})(\eta^5\text{-C}_5\text{H}_5)$  (**2**), the last-mentioned using the hyper-Rayleigh scattering technique at 1064 nm. Quadratic nonlinearities for these dppf-containing complexes are comparable to those of their dppe-containing analogues and significantly greater than carbonyl-containing analogues. The linear optical and quadratic NLO properties of **1**, **2** and their dppe-containing analogues have been rationalized by time-dependent density functional theory calculations.

© 2013 Elsevier B.V. All rights reserved.

### 1. Introduction

The nonlinear optical (NLO) properties of organometallic complexes have come under considerable scrutiny during the past twenty years [1–4], the majority of studies being focused on quadratic nonlinearities and on complexes with a donor-bridge-acceptor composition. The field of organometallics in nonlinear optics was given initial impetus from the promising outcomes of studies with metallocenyl complexes [5], but more recently alkynyl complexes have also attracted significant attention [6–8]. Amongst metal alkynyl complexes, those of ruthenium are some of the most important due to their facile high-yielding syntheses [9,10], enhanced NLO coefficients [11,12], ease of use in construction of multimetallic complexes such as dendrimers [13], and reversible redox properties which afford the possibility of NLO switching [14].

We have previously probed the effect of acceptor group incorporation and  $\pi$ -bridge modification at metal alkynyl complexes, reporting the syntheses and NLO properties (by both electric field-induced second-harmonic generation, EFISH, and the hyper-Rayleigh scattering technique, HRS) of complexes of general formula  $\text{Ru}(4\text{-C}\equiv\text{CC}_6\text{H}_4\text{X})(\text{PPh}_3)_2(\eta^5\text{-C}_5\text{H}_5)$ . Nonlinearities of these complexes increase on proceeding to a strongly dipolar system (replacing  $\text{X} = \text{H}$  by  $\text{X} = \text{NO}_2$ ) and  $\pi$ -system lengthening (proceeding from  $\text{X} = \text{NO}_2$  to  $\text{X} = \text{C}_6\text{H}_4-4\text{-NO}_2$ ,  $\text{C}\equiv\text{CC}_6\text{H}_4-4\text{-NO}_2$ ,  $\text{N}=\text{CHC}_6\text{H}_4-4\text{-NO}_2$ , and *Z*- and *E*- $\text{CH}=\text{CHC}_6\text{H}_4-4\text{-NO}_2$ , with the last-mentioned being the most efficient in terms of its quadratic NLO performance) [15–18]. We then explored the effect of metal and co-ligand variation in the series of complexes  $\text{M}(4\text{-C}\equiv\text{CC}_6\text{H}_4-4\text{-NO}_2)(\text{L}_2)(\eta^5\text{-C}_5\text{H}_5)$  ( $\text{M} = \text{Fe}, \text{Ru}, \text{Os}$ ,  $\text{L}_2 = \text{dppe}$ ;  $\text{M} = \text{Ru}, \text{Os}$ ,  $\text{L} = \text{PPh}_3$ ;  $\text{M} = \text{Ru}, \text{L} = \text{CO}$ ), for which quadratic nonlinearities increase as  $\text{M} = \text{Fe} \leq \text{Ru} \leq \text{Os}$  and  $\text{L} = \text{CO} < \text{phosphines}$  [19]. The more subtle co-ligand modification (replacing  $2 \times \text{PPh}_3$  with dppe) afforded unclear results, with  $\beta_{\text{HRS}}$  data for  $\text{M}(4\text{-C}\equiv\text{CC}_6\text{H}_4-4\text{-NO}_2)(\text{L}_2)(\eta^5\text{-C}_5\text{H}_5)$  suggesting  $(\text{M} = \text{Ru}, \text{L}_2 = 2\text{PPh}_3) < (\text{M} = \text{Ru},$

\* Corresponding author. Tel.: +61 2 6125 2927; fax: +61 2 6125 0750.  
E-mail address: [Mark.Humphrey@anu.edu.au](mailto:Mark.Humphrey@anu.edu.au) (M.G. Humphrey).

$L_2 = dppe$ ) and ( $M = Os, L_2 = 2PPh_3$ )  $\approx$  ( $M = Os, L_2 = dppe$ ) (within the error margins of the experiment). We have now returned to this question of the effect of co-ligand variation on quadratic non-linearity in metal alkynyl complexes (and thereby the potential of tuning the response), and report herein the synthesis of the new complex  $Ru(C\equiv CC_6H_4-4-NO_2)(\kappa^2-dppf)(\eta^5-C_5H_5)$  incorporating the electro-active bidentate ligand 1,2-bis(diphenylphosphino)ferrocene, structural studies of both this complex and its non-nitro analogue  $Ru(C\equiv CPh)(\kappa^2-dppf)(\eta^5-C_5H_5)$ , spectroscopic and electrochemical characterization of these complexes, quadratic non-linearities from hyper-Rayleigh scattering measurements at 1064 nm, comparison to related extant experimental data, and theoretical studies employing density functional theory (DFT) and time-dependent DFT (TD-DFT) to rationalize the experimental outcomes.

## 2. Experimental

### 2.1. General experimental conditions and starting materials

All reactions were performed under a nitrogen atmosphere with the use of Schlenk techniques unless otherwise stated. Dichloromethane was dried by distilling over calcium hydride; all other solvents were used as received. Petrol is a fraction of petroleum spirits of boiling range 60–80 °C. Chromatography was performed on ungraded basic alumina. Phenylacetylene (Aldrich) was used as received. The following were prepared by the literature procedures:  $RuCl(\kappa^2-dppf)(\eta^5-C_5H_5)$  [20],  $HC\equiv CC_6H_4-4-NO_2$  [21].

### 2.2. Instrumentation

Microanalyses were carried out at the Australian National University. UV–vis spectra of solutions in 1 cm quartz cells were recorded using a Cary 5 spectrophotometer; bands are reported in the form wavelength (nm) [extinction coefficient,  $10^4 M^{-1} cm^{-1}$ ]. The infrared spectra were recorded as KBr discs using a Perkin–Elmer System 2000 FT-IR; peaks are reported in  $cm^{-1}$ .  $^1H$  (300 MHz) and  $^{13}C$  (75 MHz) NMR spectra were recorded using an Inova-300 NMR spectrometer and  $^{31}P$  NMR spectra (121 MHz) were recorded using a Varian Mercury-300 FT NMR spectrometer. The spectra are referenced to residual chloroform (7.26 ppm),  $CDCl_3$  (77.0 ppm), or external  $H_3PO_4$  (0.0 ppm), respectively; atom labelling follows the numbering scheme in Chart 1. The high resolution ESI mass spectrum (HR ESI MS) was obtained utilizing a Bruker Apex 4.7T FTICR-MS instrument. Cyclic voltammetry measurements were recorded using a MacLab 400 interface and MacLab potentiostat from ADInstruments. The supporting electrolyte was 0.1 M ( $NBu_4$ )PF<sub>6</sub> in distilled, deoxygenated  $CH_2Cl_2$ .

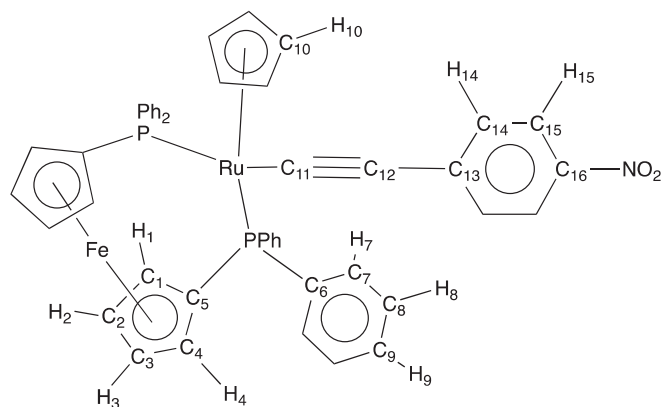


Chart 1. NMR labelling scheme for **1**.

Solutions containing ca  $1 \times 10^{-3}$  M complex were maintained under nitrogen. Measurements were carried out at room temperature using Pt disc working-, Pt wire auxiliary- and Ag/AgCl reference electrodes, such that the ferrocene/ferrocenium redox couple was located at 0.56 V (peak separation ca. 0.10 V). Scan rates were typically  $100 mV s^{-1}$ .

### 2.3. Synthesis of $Ru(C\equiv CC_6H_4-4-NO_2)(\kappa^2-dppf)(\eta^5-C_5H_5)$ (**1**)

$RuCl(\kappa^2-dppf)(\eta^5-C_5H_5)$  (210.2 mg, 0.278 mmol) and  $HC\equiv CC_6H_4-4-NO_2$  (41.5 mg, 0.282 mmol) were added to a flask containing MeOH (20 ml). A solution of NaOMe in MeOH (7.00 ml, 0.1 M) was added and the orange mixture was stirred at reflux until the formation of a red solution (ca. 15 min). The red solution was cooled to room temperature, resulting in the precipitation of a red powder that was collected by filtration, affording **1** (184.3 mg, 77%). Crystals of **1** suitable for single-crystal X-ray structural study were grown by slow diffusion of methanol into a dichloromethane solution at room temperature. Elemental analysis ( $C_{47}H_{37}FeNO_2 \cdot P_2Ru$ ): calcd.: C: 65.14, H: 4.30, N: 1.62%. Found: C: 65.30, H: 4.18, N: 1.35%. HR ESI MS ( $C_{47}H_{37}FeNO_2P_2Ru$ ): calculated: 882.0927, found: 882.0944. UV–vis ( $CH_2Cl_2$ ): 469 nm (1.74), 273 nm (1.42).  $^1H$  NMR ( $CDCl_3$ ): 3.95, 4.04, 4.11, 5.06 (4 s,  $4 \times 2H, H_1, H_2, H_3, H_4$ ), 4.27 (s, 5H,  $H_{10}$ ), 7.08 (d,  $J_{HH} = 9 Hz, 2H, H_{14}$ ), 7.18–7.73 (m, 20H,  $H_7, H_8, H_9$ ), 7.99 (d,  $J_{HH} = 9 Hz, 2H, H_{15}$ ).  $^{13}C$  NMR ( $CDCl_3$ ): 68.3, 71.3, 73.2, 76.0 ( $C_1, C_2, C_3, C_4$ ), 80.8 ( $C_{12}$ ), 85.0 ( $C_{10}$ ), 88.3 (t,  $J_{CP} = 35 Hz, C_5$ ), 115.6 ( $C_{11}$ ), 123.9 ( $C_{14}$ ), 127.3 (m), 128.8, 129.3, 134.0 (m) ( $C_7, C_8, C_9$ ), 130.5 ( $C_{15}$ ), 137.5 ( $C_{13}$ ), 140.4 (m,  $C_6$ ), 142.7 ( $C_{16}$ ).  $^{31}P$  NMR ( $CDCl_3$ ): 55.9.

### 2.4. Synthesis of $Ru(C\equiv CPh)(\kappa^2-dppf)(\eta^5-C_5H_5)$ (**2**)

This complex has been prepared previously by an alternative procedure in 98% yield [22].  $RuCl(\kappa^2-dppf)(\eta^5-C_5H_5)$  (113.7 mg, 0.15 mmol) and  $HC\equiv CPh$  (0.05 ml, 0.46 mmol) were added to a flask containing MeOH (15 ml). A solution of NaOMe in MeOH (7.00 ml, 0.1 M) was added and the orange mixture was stirred at reflux until the formation of a red solution (ca. 15 min). The red solution was cooled to room temperature, resulting in the precipitation of a yellow powder that was collected by filtration, affording **2** (103.0 mg, 83%). Crystals of **2** suitable for X-ray diffraction study were grown by slow diffusion of methanol into a dichloromethane solution at room temperature. UV–vis ( $CH_2Cl_2$ ): 402 nm (0.14), 311 nm (2.18), 273 nm (1.36).  $^{31}P$  NMR ( $CDCl_3$ ): 56.0.

### 2.5. Structure determinations

Intensity data were collected using an Enraf-Nonius KAPPA CCD at 200 K with Mo  $K\alpha$  radiation ( $\lambda = 0.7170 \text{ \AA}$ ). Suitable crystals were immersed in viscous hydrocarbon oil and mounted on a glass fibre that was mounted on the diffractometer. Using psi and omega scans  $N_t$  (total) reflections were measured, which were reduced to  $N_o$  unique reflections, with  $F_o > 2\sigma(F_o)$  being considered “observed”. Data were initially processed and corrected for absorption using the programs DENZO [23] and SORTAV [24]. The structures were solved using direct methods, and observed reflections were used in least squares refinement on  $F^2$ , with anisotropic thermal parameters refined for non-hydrogen atoms. Hydrogen atoms were constrained in calculated positions and refined with a riding model. Structure solutions and refinements were performed using the programs SHELXS-97 and SHELXL-97 [25] through the graphical interface Olex2 [26], which was also used to generate the figures. Crystal data for **1**:  $C_{47}H_{37}FeNO_2P_2Ru$ ,  $M = 866.64$ , red block,  $0.10 \times 0.10 \times 0.09 mm^3$ , triclinic, space group  $P-1$  (no. 2),  $a = 9.926(2)$ ,  $b = 12.406(3)$ ,  $c = 15.571(3) \text{ \AA}$ ,  $\alpha = 97.23(3)$ ,

$\beta = 99.29(3)$ ,  $\gamma = 99.36(3)^\circ$ ,  $V = 1844.1(6) \text{ \AA}^3$ ,  $Z = 2$ ,  $D_c = 1.561 \text{ g/cm}^3$ ,  $F_{000} = 884$ ,  $\mu = 0.933 \text{ mm}^{-1}$ ,  $2\theta_{\text{max}} = 55.0^\circ$ , 35,613 reflections collected, 8438 unique ( $R_{\text{int}} = 0.0358$ ). Final  $\text{GoF} = 1.192$ ,  $R1 = 0.0278$ ,  $wR2 = 0.0813$ ,  $R$  indices based on 7392 reflections with  $I > 2\sigma(I)$  (refinement on  $F^2$ ), 487 parameters, 0 restraints. Crystal data for  $2 \cdot \text{CH}_2\text{Cl}_2$ :  $\text{C}_{48}\text{H}_{40}\text{Cl}_2\text{FeP}_2\text{Ru}$ ,  $M = 906.56$ , yellow block,  $0.12 \times 0.10 \times 0.09 \text{ mm}^3$ , monoclinic, space group  $P2_1/n$  (No. 14),  $a = 10.232(2)$ ,  $b = 23.572(5)$ ,  $c = 17.482(4) \text{ \AA}$ ,  $\beta = 93.51(3)^\circ$ ,  $V = 4208.7(14) \text{ \AA}^3$ ,  $Z = 4$ ,  $D_c = 1.431 \text{ g/cm}^3$ ,  $F_{000} = 1848$ ,  $\mu = 0.939 \text{ mm}^{-1}$ ,  $2\theta_{\text{max}} = 55.8^\circ$ , 60,857 reflections collected, 9777 unique ( $R_{\text{int}} = 0.0538$ ). Final  $\text{GoF} = 1.063$ ,  $R1 = 0.0839$ ,  $wR2 = 0.2449$ ,  $R$  indices based on 7119 reflections with  $I > 2\sigma(I)$  (refinement on  $F^2$ ), 500 parameters, 156 restraints. CCDC 899522–899523. *Variata*. For compound **2**, atoms C41–C47 of the phenylalkynyl moiety exhibited positional disorder. This disorder was successfully modelled using a two-position model with 0.49894(0.00707):0.50106 occupancy levels, in conjunction with geometry restraints. The anisotropic displacement parameters of these atoms were also restrained. The unit cell of **2** contains four dichloromethane molecules that have been treated as a diffuse contribution to the overall scattering without specific atom positions by PLATON SQUEEZE [27].

## 2.6. Hyper-Rayleigh scattering measurements

An injection-seeded Nd:YAG laser (Q-switched Nd:YAG Quanta Ray GCR5, 1.064  $\mu\text{m}$ , 8 ns pulses, 10 Hz) was focused into a cylindrical cell (7 ml) containing the sample. The intensity of the incident beam was varied by rotation of a half-wave plate placed between crossed polarizers. Part of the laser pulse was sampled by a photodiode to measure the vertically polarized incident light intensity. The frequency doubled light was collected by an efficient condenser system and detected by a photomultiplier. The harmonic scattering and linear scattering were distinguished by appropriate filters; gated integrators were used to obtain intensities of the incident and harmonic scattered light. The absence of a luminescence contribution to the harmonic signal was confirmed by using interference filters at different wavelengths near 532 nm. All measurements were performed in tetrahydrofuran using 4-nitroaniline ( $\beta = 21.4 \times 10^{-30}$  esu) as a reference. Reported  $\beta$  values were obtained using the so-called “B convention”, which incorporates the 1/2! and 1/3! factors from the Taylor series expansion. Solutions were sufficiently dilute that absorption of scattered light was negligible. Further details regarding ns HRS studies employing a Nd:YAG laser are given in Refs. [28] and [29].

## 2.7. Theoretical studies

Calculations were performed using the Amsterdam Density Functional (ADF) program [30], version ADF2012.01. Scalar relativistic effects were treated via the zeroth-order regular approximation (ZORA) method [31]. Geometry optimizations were undertaken without any symmetry constraints using the Becke–Perdew (BP) exchange–correlation [32–34] functional with triple

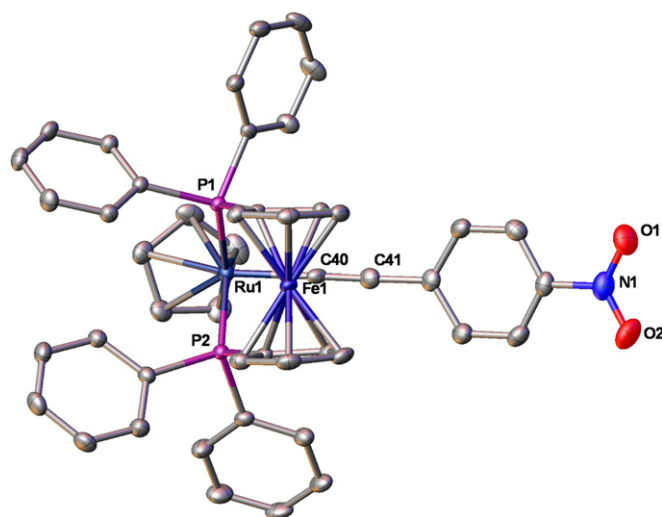


**Fig. 1.** Molecular structure of  $\text{Ru}(\text{C}\equiv\text{CC}_6\text{H}_4\text{-4-NO}_2)(\kappa^2\text{-dppf})(\eta^5\text{-C}_5\text{H}_5)$  (**1**), with thermal ellipsoids set at the 30% probability level. Hydrogen atoms have been omitted for clarity. Selected bond lengths and angles:  $\text{Ru}-\text{C}_{40}$  2.033(2),  $\text{Ru}-\text{P}_1$  2.282(1),  $\text{Ru}-\text{P}_2$  2.283(1),  $\text{C}_{40}\equiv\text{C}_{41}$  1.186(3),  $\text{C}_{41}-\text{C}_{42}$  1.434(3)  $\text{ \AA}$ ,  $\text{Ru}-\text{C}_{40}\equiv\text{C}_{41}$  178.4(2),  $\text{C}_{40}\equiv\text{C}_{41}-\text{C}_{42}$  167.3(3),  $\text{P}_1-\text{Ru}-\text{P}_2$  95.93(3) $^\circ$ .

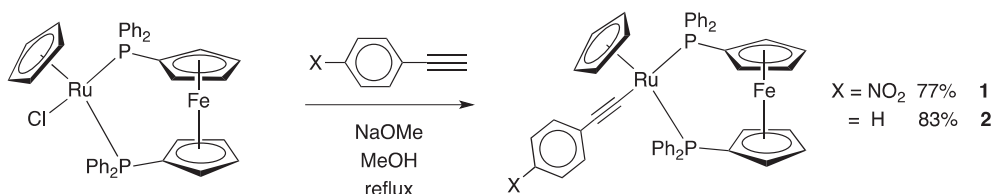
zeta plus polarization (TZP) Slater orbital basis sets for all atoms. UV–vis spectra were calculated using the statistical average of orbital potentials (SAOP) functional [35] with the same TZP basis sets. Calculated  $\beta$  values were obtained using the Taylor series convention. For clarity, the approximate location of the Cartesian axes for the calculations are (with reference to Fig. 1)  $\text{Ru1}-\text{C}_{40}-\text{C}_{41}-\text{N1}$  ( $x$  axis), and through  $\text{Ru1}$  and orthogonal to the plane of the figure ( $z$  axis), with the  $y$  axis orthogonal to these  $x$  and  $z$  axes.

## 3. Results and discussion

### 3.1. Synthesis and characterization

The alkyne complexes were prepared using extensions of established methodologies (Scheme 1), and the new complex **1** was characterized by a combination of IR,  $^1\text{H}$ ,  $^{13}\text{C}$ , and  $^{31}\text{P}$  NMR spectroscopies and mass spectrometry. The IR spectra contain characteristic  $\nu(\text{C}\equiv\text{C})$  bands at 2039 (**1**) and 2073  $\text{cm}^{-1}$  (**2**) for the stretching mode of the metal-bound alkyne group, with the anticipated shift to lower frequency on introduction of a nitro group. The  $^{31}\text{P}$  NMR spectra contain one singlet resonance at 55.9 (**1**) and 56.0 ppm (**2**), while the high resolution mass spectrum of **1** shows a peak corresponding to the molecular ion.

We have previously reported the cyclic voltammetric response of complexes of general formula  $\text{Ru}(\text{C}\equiv\text{CC}_6\text{H}_4\text{-4-NO}_2)(\text{L}_2)(\eta^5\text{-C}_5\text{H}_5)$ , for which the potentials of the formally  $\text{Ru}^{\text{II/III}}$  oxidation processes increase on proceeding from  $\text{L}_2 = \text{dppe}$  (0.67 V) [19] to  $(\text{PPh}_3)_2$  (0.73 V) [15] and then  $(\text{CO})_2$  (0.86 V) [19], consistent with



**Scheme 1.** Syntheses of ruthenium alkyne complexes **1** and **2**.

expectations of decreasing electron density at the metal centre in proceeding from electron-donating alkylidynylphosphines to triarylphosphines and then electron-withdrawing carbonyl ligands. Complex **1** was investigated in the same way, revealing two oxidation processes [ $\text{Fe}^{\text{II/III}}$  0.73 V;  $\text{Ru}^{\text{II/III}}$  1.00 V], the dppe ligand-centred oxidation rendering the ruthenium centre considerably more difficult to oxidize. Redox switching of optical nonlinearities has attracted significant attention [36,37]. The reversible stepwise oxidation of **1** suggests that this complex may have potential in this regard because the donor nature of the ligated ruthenium centre in this formally donor-bridge-acceptor composition will be attenuated or “switched off” following oxidation, which should lead to a diminution of quadratic optical nonlinearity.

The identities of **1** and **2** were confirmed by single-crystal X-ray diffraction studies; the molecular structures are illustrated in Figs. 1 and 2, the captions including selected bond lengths and angles which fall within the ranges of those reported previously for related structures. Full bond lengths and angles are provided in Supplementary material.

### 3.2. Linear optical and quadratic nonlinear optical studies

Absorption maxima and intensities from electronic spectra of **1** and **2**, together with those of related complexes, are collected in Table 1. We have previously assigned the low-energy transitions in ruthenium alkynyl complexes of this type as metal-to-ligand charge transfer (MLCT) in character [15]. The two-level model suggests that strong low-energy transitions involving significant charge displacement (such as the MLCT transitions for these complexes) are correlated with significant quadratic nonlinearity, so understanding the effect of systematic complex modification on  $\lambda_{\text{max}}$  and  $\epsilon$  are important. For these complexes, introduction of a nitro group (and thereby creating a strong donor-bridge-acceptor composition) results in a significant red-shift of the optical absorption maximum from ca. 310 nm to ca. 460 nm; there is a concomitant slight reduction in the extinction

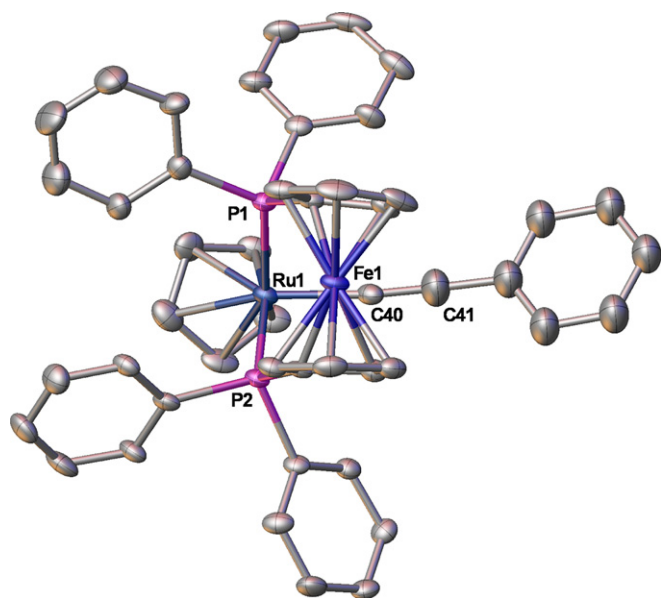


**Fig. 2.** Molecular structure of  $\text{Ru}(\text{C}\equiv\text{CPh})(\kappa^2\text{-dppf})(\eta^5\text{-C}_5\text{H}_5)$  (**2**), with thermal ellipsoids set at the 30% probability level. Hydrogen atoms and the disorder component of the phenylalkynyl moiety have been omitted for clarity. Selected bond lengths and angles:  $\text{Ru}-\text{C}_{40}$  2.015(8),  $\text{Ru}-\text{P}_1$  2.272(2),  $\text{Ru}-\text{P}_2$  2.273(2),  $\text{C}_{40}\equiv\text{C}_{41}$  1.26(5),  $\text{C}_{41}-\text{C}_{42}$  1.49(5) Å,  $\text{Ru}-\text{C}_{40}\equiv\text{C}_{41}$  173(3),  $\text{C}_{40}\equiv\text{C}_{41}-\text{C}_{42}$  161(5),  $\text{P}_1-\text{Ru}-\text{P}_2$  96.87(6)°.

**Table 1**

Experimental linear optical and quadratic nonlinear response parameters for **1**, **2** and related complexes.

Complex	$\lambda_{\text{max}}$ (nm) [ $\epsilon$ , $10^4 \text{ M}^{-1} \text{ cm}^{-1}$ ] <sup>a</sup>	$\beta_{1064}$ ( $10^{-30} \text{ esu}$ ) <sup>b</sup>	$\beta_0$ ( $10^{-30} \text{ esu}$ ) <sup>c</sup>	Ref.
$\text{Ru}(\text{C}\equiv\text{CPh})(\text{PPh}_3)_2$ ( $\eta^5\text{-C}_5\text{H}_5$ )	310 [2.0]	16	10	[15]
$\text{Ru}(\text{C}\equiv\text{CPh})(\text{dppf})$ ( $\eta^5\text{-C}_5\text{H}_5$ ) ( <b>2</b> )	311 [2.2]	120	72	This work
$\text{Ru}(4\text{-C}\equiv\text{CC}_6\text{H}_4\text{NO}_2)$ ( $\text{PPh}_3$ ) <sub>2</sub> ( $\eta^5\text{-C}_5\text{H}_5$ )	460 [1.1]	468	96	[15]
$\text{Ru}(4\text{-C}\equiv\text{CC}_6\text{H}_4\text{NO}_2)$ ( $\text{CO}$ ) <sub>2</sub> ( $\eta^5\text{-C}_5\text{H}_5$ )	364 [1.6]	58	27	[19]
$\text{Ru}(4\text{-C}\equiv\text{CC}_6\text{H}_4\text{NO}_2)$ (dppe)( $\eta^5\text{-C}_5\text{H}_5$ )	447 [1.8]	664	161	[19]
$\text{Ru}(4\text{-C}\equiv\text{CC}_6\text{H}_4\text{NO}_2)$ (dppf)( $\eta^5\text{-C}_5\text{H}_5$ ) ( <b>1</b> )	469 [1.7]	770	165	This work

<sup>a</sup> Dichloromethane solvent.

<sup>b</sup> Measurements were carried out in THF; all complexes are optically transparent at 1064 nm. Errors  $\pm 10\%$ .

<sup>c</sup> Corrected for resonance enhancement at 532 nm using the two-level model with  $\beta_0 = \beta[1 - (2\lambda_{\text{max}}/1064)^2][1 - (\lambda_{\text{max}}/1064)^2]$ .

coefficient, perhaps indicating the presence of another transition contributing to the band at ca. 310 nm in the spectra of the non-nitro complexes. Amongst the nitro-containing complexes, replacing the (comparatively) electron-withdrawing carbonyl ligands with electron-donating phosphines results in a significant red-shift in  $\lambda_{\text{max}}$ .

The quadratic nonlinearities of **1** and **2** have been determined at 1064 nm using the hyper-Rayleigh scattering technique; the results are given in Table 1, together with the two-level corrected values, and data for related complexes. Problems with the two-level model have been discussed previously by us [38]; while it is not considered adequate for donor-bridge-acceptor organometallics such as those in this report, it may be useful in comparing closely related complexes. With this caveat in mind, one can compare the data. Both experimental and two-level corrected nonlinearities increase significantly on proceeding from non-nitro to nitro-containing complexes (as expected when replacing a donor-bridge with a donor-bridge-acceptor composition). For the nitro-containing complexes, experimental and two-level corrected data undergo substantial increase on proceeding from electron-withdrawing co-ligand CO to electron-donating triphenylphosphine with a further increase seen in proceeding to the bidentate diphosphines. The dppe complexes from the present study are of particular interest; they possibly exhibit the largest nonlinearities within this family of complexes (although the experimental and two-level-corrected data for **1** are comparable to those of its dppe-containing analogue within experimental error margins). Coupled to their aforementioned redox activity, they afford the intriguing possibility of redox switching the quadratic NLO performance by sequential oxidation at the ferrocenyl unit and then the ruthenium centre.

### 3.3. Theoretical studies

TD-DFT calculations of **1**, **2**, and their dppe-containing analogues were undertaken to rationalize the linear optical and quadratic nonlinear optical behaviours. Although the TD-DFT calculations computed the 200 lowest energy dipole-allowed excitations for each complex, in general only transitions with calculated oscillator strengths of 0.04 atomic units or greater below  $35,000 \text{ cm}^{-1}$  were considered in the analysis to follow. The calculated transition energies, oscillator strengths [ $f$ ], and main orbital contributions involved in the excitations are listed in Table 2 for all four

**Table 2**  
Observed and calculated optical transitions for **1**, **2**, Ru(C≡CPh)(dppe)(η<sup>5</sup>-C<sub>5</sub>H<sub>5</sub>) and Ru(4-C≡CC<sub>6</sub>H<sub>4</sub>NO<sub>2</sub>)(dppe)(η<sup>5</sup>-C<sub>5</sub>H<sub>5</sub>).<sup>a</sup>

Complex	$\nu_{\max}$ [ $\epsilon$ ] (exp)	$\nu_{\max}$ [ $f$ ] (calcd)	Composition (wt%)	Major assignment
Ru(C≡CPh)(dppe)(η <sup>5</sup> -C <sub>5</sub> H <sub>5</sub> )	30,950 [1.91]	28,280 [0.09] 29,952 [0.19] 30,637 [0.07]	170a → 180a (51%) 170a → 180a (36%) 170a → 181a (81%)	Ru <sub>dxz</sub> + πC <sub>2</sub> → Ru <sub>dyz</sub> + π <sup>*</sup> C <sub>2</sub> Ph Ru <sub>dxz</sub> + πC <sub>2</sub> → Ru <sub>dyz</sub> + π <sup>*</sup> C <sub>2</sub> Ph Ru <sub>dxz</sub> + πC <sub>2</sub> → Ru <sub>dyz</sub> + π <sup>*</sup> C <sub>2</sub> Ph + P <sub>yz</sub>
Ru(4-C≡CC <sub>6</sub> H <sub>4</sub> NO <sub>2</sub> )(dppe)(η <sup>5</sup> -C <sub>5</sub> H <sub>5</sub> )	20,500 [1.58] 32,550 [0.68]	17,600 [0.47] 26,392 [0.06] 29,467 [0.07] 32,066 [0.04] 32,434 [0.08]	182a → 183a (89%) 179a → 183a (61%) 173a → 183a (41%) 179a → 185a (45%) 181a → 194a (40%)	Ru <sub>dxz-y2</sub> + P <sub>yz</sub> + πC <sub>2</sub> C <sub>6</sub> H <sub>4</sub> NO <sub>2</sub> → π <sup>*</sup> C <sub>2</sub> C <sub>6</sub> H <sub>4</sub> NO <sub>2</sub> Ru <sub>dxz-y2</sub> + πC <sub>2</sub> C <sub>6</sub> H <sub>4</sub> NO <sub>2</sub> + πCp → π <sup>*</sup> C <sub>2</sub> C <sub>6</sub> H <sub>4</sub> NO <sub>2</sub> π(dppe) → π <sup>*</sup> C <sub>2</sub> C <sub>6</sub> H <sub>4</sub> NO <sub>2</sub> Ru <sub>dxz-y2</sub> + πC <sub>2</sub> C <sub>6</sub> H <sub>4</sub> NO <sub>2</sub> + πCp → Ru <sub>dxz</sub> + π <sup>*</sup> dppe Ru <sub>dxz</sub> + πC <sub>2</sub> → Ru <sub>dxz</sub> + π <sup>*</sup> C <sub>2</sub> C <sub>6</sub> H <sub>4</sub> NO <sub>2</sub>
Ru(C≡CPh)(dppf)(η <sup>5</sup> -C <sub>5</sub> H <sub>5</sub> ) ( <b>2</b> )	24,500 [0.15] 32,150 [2.82]	24,077 [0.01] 25,547 [0.01] 29,368 [0.05] 29,864 [0.04] 31,511 [0.05] 31,659 [0.06]	207a → 213a (83%) 206a → 213a (92%) 207a → 221a (37%) 206a → 219a (17%) 205a → 216a (15%) 210a → 224a (12%) 204a → 212a (58%) 206a → 221a (37%)	Fe <sub>dz2</sub> + Ru <sub>dxz</sub> → π <sup>*</sup> (dppe) Fe <sub>dz2</sub> + Ru <sub>dxz</sub> → π <sup>*</sup> (dppe) Fe <sub>dz2</sub> + Ru <sub>dxz</sub> → π <sup>*</sup> C <sub>2</sub> Ph Fe <sub>dz2/dxz2-y2</sub> + Ru <sub>dxz2-y2</sub> → Fe <sub>dxz</sub> + π <sup>*</sup> (dppe) Fe <sub>dxz2-y2</sub> → Fe <sub>dyz</sub> + Ru <sub>dyz</sub> + π <sup>*</sup> (dppe) Ru <sub>dz2</sub> + πC <sub>2</sub> Ph → Ru <sub>dxz</sub> + π <sup>*</sup> Cp Ru <sub>dz2</sub> + πC <sub>2</sub> Ph → π <sup>*</sup> (dppe) Fe <sub>dz2</sub> + Ru <sub>dxz2-y2</sub> → π <sup>*</sup> C <sub>2</sub> Ph
Ru(4-C≡CC <sub>6</sub> H <sub>4</sub> NO <sub>2</sub> )(dppf)(η <sup>5</sup> -C <sub>5</sub> H <sub>5</sub> ) ( <b>1</b> )	21,160 [3.02] 34,000 [2.20]	19,028 [0.35] 27,846 [0.04] 32,031 [0.08] 34,773 [0.07]	219a → 222a (39%) 206a → 222a (47%) 199a → 222a (57%) 216a → 236a (28%)	Ru <sub>dz2</sub> + Fe <sub>dz2</sub> + πC <sub>2</sub> C <sub>6</sub> H <sub>4</sub> NO <sub>2</sub> → π <sup>*</sup> C <sub>2</sub> C <sub>6</sub> H <sub>4</sub> NO <sub>2</sub> O <sub>px</sub> + πC <sub>2</sub> + π(dppe) → π <sup>*</sup> C <sub>2</sub> C <sub>6</sub> H <sub>4</sub> NO <sub>2</sub> Ru <sub>dxz</sub> + πC <sub>2</sub> C <sub>6</sub> H <sub>4</sub> NO <sub>2</sub> + πCp → π <sup>*</sup> C <sub>2</sub> C <sub>6</sub> H <sub>4</sub> NO <sub>2</sub> Fe <sub>dxz2-y2</sub> + Ru <sub>dxz2-y2</sub> → Ru <sub>dxz</sub> + π <sup>*</sup> C <sub>2</sub> C <sub>6</sub> H <sub>4</sub> NO <sub>2</sub>

<sup>a</sup> Calculated and observed  $\nu_{\max}$  in cm<sup>-1</sup>; [ $\epsilon$ ] in 10<sup>4</sup> M<sup>-1</sup> cm<sup>-1</sup>; calcd oscillator strength [ $f$ ].

complexes along with the observed band positions. The position and relative intensities (depicted as vertical lines) of the calculated transitions are also shown alongside the experimental UV–vis spectra in Fig. 3. Plots of the main occupied and virtual molecular orbitals involved in the calculated transitions are shown in Fig. 4.

The calculated absorption spectra indicate that there is negligible spectral intensity below 17,000 and 28,000 cm<sup>-1</sup>, respectively, for the nitro and non-nitro substituted species, in agreement with

the experimental spectra. The introduction of the nitro substituent on the axial phenyl group results in a red-shift of the main lowest energy band in the experimental spectra between 10,000 and 11,000 cm<sup>-1</sup> for **1** and Ru(4-C≡CC<sub>6</sub>H<sub>4</sub>NO<sub>2</sub>)(dppe)(η<sup>5</sup>-C<sub>5</sub>H<sub>5</sub>), and this shift is nicely reproduced in the calculated spectra. Based on the observed band positions for Ru(C≡CPh)(dppe)(η<sup>5</sup>-C<sub>5</sub>H<sub>5</sub>) and **2**, and also their nitro-substituted analogues Ru(4-C≡CC<sub>6</sub>H<sub>4</sub>NO<sub>2</sub>)(dppe)(η<sup>5</sup>-C<sub>5</sub>H<sub>5</sub>) and **1**, it appears that replacing

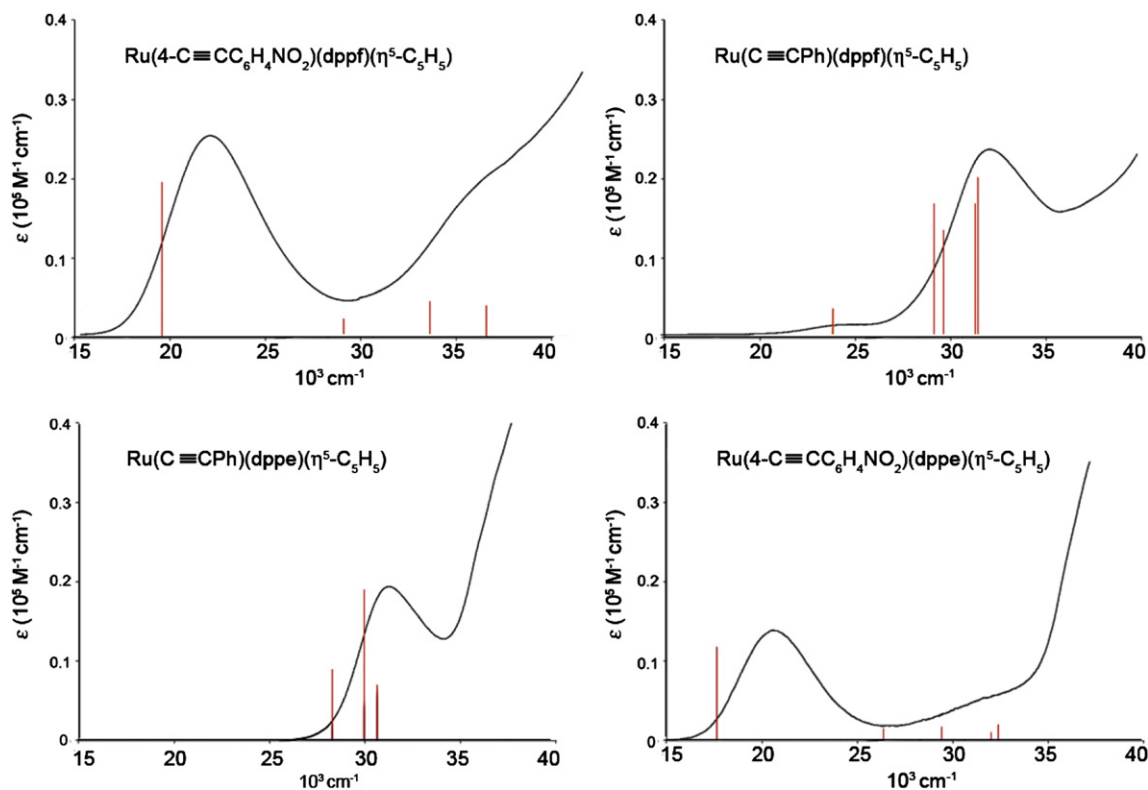


**Fig. 3.** Calculated and experimental absorption spectra for **1** (top left), **2** (top right), Ru(C≡CPh)(dppe)(η<sup>5</sup>-C<sub>5</sub>H<sub>5</sub>) (bottom left) and Ru(4-C≡CC<sub>6</sub>H<sub>4</sub>NO<sub>2</sub>)(dppe)(η<sup>5</sup>-C<sub>5</sub>H<sub>5</sub>) (bottom right).

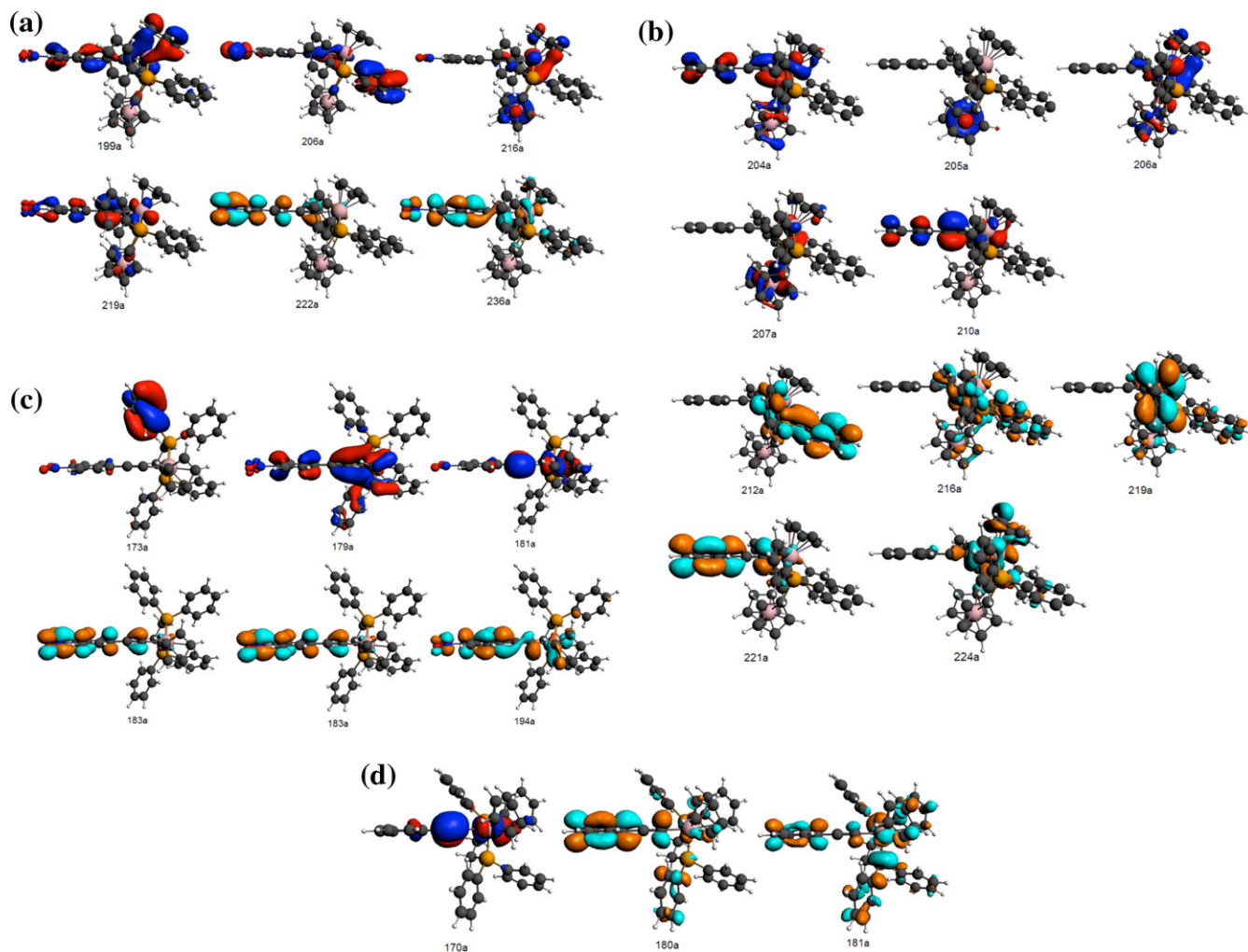


**Fig. 4.** Major occupied and virtual molecular orbitals involved in the calculated transitions for (a) **1**, (b) **2**, (c) Ru(4-C≡CC<sub>6</sub>H<sub>4</sub>NO<sub>2</sub>)(dppe)(η<sup>5</sup>-C<sub>5</sub>H<sub>5</sub>), and (d) Ru(C≡CPh)(dppe)(η<sup>5</sup>-C<sub>5</sub>H<sub>5</sub>).

the dppe ligand by dppf has only a minor effect, at least for the lowest energy transitions, and this is borne out in the calculated spectra in that these bands have only minor contributions from the phosphine-based donor ligands.

On the basis of the data in Table 2, the main band at around 31,000 cm<sup>-1</sup> for Ru(C≡CPh)(dppe)(η<sup>5</sup>-C<sub>5</sub>H<sub>5</sub>) can be assigned to transitions originating from the 170a orbital, dominated by Ru<sub>d<sub>xz</sub></sub> and C<sub>2</sub> π character, to the 180a or 181a π\* orbitals which are mostly localized on the C<sub>2</sub>Ph fragment. For the corresponding nitro substituted complex Ru(4-C≡CC<sub>6</sub>H<sub>4</sub>NO<sub>2</sub>)(dppe)(η<sup>5</sup>-C<sub>5</sub>H<sub>5</sub>), the lowest energy band is red-shifted, as noted above, but can be attributed to a transition from the 182a orbital possessing Ru<sub>d<sub>x<sup>2</sup>-y<sup>2</sup></sub></sub> and C<sub>2</sub>C<sub>6</sub>H<sub>4</sub>NO<sub>2</sub> π character, to the 183a orbital which is mostly of C<sub>2</sub>C<sub>6</sub>H<sub>4</sub>NO<sub>2</sub> π\* character. In the case of the dppf complex **2**, the main band at approximately 32,500 cm<sup>-1</sup> is assigned to transitions from the 204a, 206a and 207a orbitals, comprising a mixture of Ru<sub>d<sub>z<sup>2</sup></sub></sub>/d<sub>x<sup>2</sup>-y<sup>2</sup></sub>, Fe<sub>d<sub>z<sup>2</sup></sub></sub> and C<sub>2</sub>Ph π character, to the 212a, 219a and 221a levels which are primarily π\* orbitals on either the C<sub>2</sub>Ph fragment or dppf ligand. For complex **1**, the main (red-shifted) band at around 21,000 cm<sup>-1</sup> is assigned to a transition from the 219a orbital, comprising Ru/Fe<sub>d<sub>z<sup>2</sup></sub></sub> and C<sub>2</sub>C<sub>6</sub>H<sub>4</sub>NO<sub>2</sub> π character, to the 222a orbital which is primarily of C<sub>2</sub>C<sub>6</sub>H<sub>4</sub>NO<sub>2</sub> π\* character.

In addition, for the nitro-substituted complexes, **1** and Ru(4-C≡CC<sub>6</sub>H<sub>4</sub>NO<sub>2</sub>)(dppe)(η<sup>5</sup>-C<sub>5</sub>H<sub>5</sub>), several weak bands are observed

to higher energy, in the vicinity of 26,000 to 35,000 cm<sup>-1</sup>, which can be assigned to transitions arising from orbitals with Ru, C<sub>2</sub>C<sub>6</sub>H<sub>4</sub>NO<sub>2</sub> π and Cp π character to orbitals largely localized on the C<sub>2</sub>C<sub>6</sub>H<sub>4</sub>NO<sub>2</sub> fragment. A very weak band is observed around 24,500 cm<sup>-1</sup> in complex **2** which, on the basis of the calculations, can be attributed primarily to an internal charge transfer transition on the dppf ligand. A similar weak band in the vicinity of 23,500 cm<sup>-1</sup> is also predicted for the corresponding nitro-substituted complex **1** but, presumably, is obscured by the main lowest energy band now positioned at approximately 22,000 cm<sup>-1</sup> due to the red-shift noted above.

The first hyperpolarizability, β, is a third rank tensor with 27 components. Application of Kleinman symmetry [39] reduces the number of unique components, allowing β to be calculated from the following expression:

$$\beta_{\text{tot}} = \left[ (\beta_{xxx} + \beta_{xyy} + \beta_{xzz})^2 + (\beta_{yyy} + \beta_{yzz} + \beta_{yxx})^2 + (\beta_{zzz} + \beta_{zxx} + \beta_{zyy})^2 \right]^{1/2} \quad (1)$$

The calculated components of β and resulting β<sub>tot</sub> value based on the above equation are listed in Table 3 along with the experimental value β<sub>0,exp</sub> that is obtained from the frequency dependent β value measured at 1064 nm using the two-level approximation [5]:

**Table 3**Calculated and observed NLO data for **1**, **2**, Ru(C≡CPh)(dppe)(η<sup>5</sup>-C<sub>5</sub>H<sub>5</sub>) and Ru(4-C≡CC<sub>6</sub>H<sub>4</sub>NO<sub>2</sub>)(dppe)(η<sup>5</sup>-C<sub>5</sub>H<sub>5</sub>).<sup>a</sup>

Complex	β <sub>xxx</sub>	β <sub>xyy</sub>	β <sub>xzz</sub>	β <sub>yyy</sub>	β <sub>yzz</sub>	β <sub>yxx</sub>	β <sub>zzz</sub>	β <sub>zxx</sub>	β <sub>zyy</sub>	β <sub>tot</sub>	β <sub>0,exp</sub>
Ru(C≡CPh)(dppe)(η <sup>5</sup> -C <sub>5</sub> H <sub>5</sub> )	-11.8	-1.6	1.0	-8.0	-0.2	13.2	1.1	7.7	4.7	19.0	
Ru(4-C≡CC <sub>6</sub> H <sub>4</sub> NO <sub>2</sub> )(dppe)(η <sup>5</sup> -C <sub>5</sub> H <sub>5</sub> )	-114.5	-19.5	-4.7	4.1	2.7	55.3	1.0	36.0	6.9	158.2	161
Ru(C≡CPh)(dppf)(η <sup>5</sup> -C <sub>5</sub> H <sub>5</sub> ) ( <b>2</b> )	-8.3	-0.7	0.0	-0.8	0.4	9.5	-1.1	6.4	0.0	13.8	72
Ru(4-C≡CC <sub>6</sub> H <sub>4</sub> NO <sub>2</sub> )(dppf)(η <sup>5</sup> -C <sub>5</sub> H <sub>5</sub> ) ( <b>1</b> )	-109.2	-14.2	-8.6	2.5	3.5	48.9	0.6	36.7	3.6	148.7	165

<sup>a</sup> Calculated and observed β in units of 10<sup>-30</sup> esu; β<sub>tot</sub> determined from equation (1); β<sub>0,exp</sub> evaluated using equation (2) (see Table 1).

$$\beta_{0,exp} = \beta_{exp} \left[ 1 - (\lambda_{max}/1064)^2 \right] \left[ 1 - (2\lambda_{max}/1064)^2 \right] \quad (2)$$

Addition of the nitro group on the axial phenylalkynyl fragment in both complexes **1** and Ru(4-C≡CC<sub>6</sub>H<sub>4</sub>NO<sub>2</sub>)(dppe)(η<sup>5</sup>-C<sub>5</sub>H<sub>5</sub>) results in an increase in the calculated β<sub>tot</sub> values of between 135 and 140 × 10<sup>-30</sup> esu. While the same level of enhancement is not evident in the experimental data for the dppf complex (**1**), a significant increase of 93 × 10<sup>-30</sup> esu in β<sub>0,exp</sub> is nonetheless observed, which is consistent with other related group 8 metal alkynyl systems in which a nitro substituent has been introduced on the axial phenylalkynyl group [8].

Although none of the four complexes possess any symmetry, a pseudo mirror plane exists in the xz plane, bisecting the Ru centre, C<sub>2</sub>Ph/C<sub>2</sub>C<sub>6</sub>H<sub>4</sub>NO<sub>2</sub> group and the Cp ring. Consequently, the calculated values for β<sub>yyy</sub> and β<sub>zzz</sub> are close to zero. For complexes **1** and Ru(4-C≡CC<sub>6</sub>H<sub>4</sub>NO<sub>2</sub>)(dppe)(η<sup>5</sup>-C<sub>5</sub>H<sub>5</sub>), the presence of the nitro substituent provides a dominant donor–acceptor pathway from the Ru centre along the phenylalkynyl axis for charge to be delocalized. This charge transfer pathway lies approximately in the xz plane but has its major component along the molecular x axis. Consequently, for these two complexes the diagonal β<sub>xxx</sub> component contributes most to β<sub>tot</sub>, followed next by the non-diagonal β<sub>xyy</sub> and β<sub>xzz</sub> components which contribute less than half of the magnitude of β<sub>xxx</sub>. This picture is confirmed from the orbital contributions given in Table 2. The lowest energy band in these complexes is dominated by a single transition, 182a → 183a and 219a → 222a, for Ru(4-C≡CC<sub>6</sub>H<sub>4</sub>NO<sub>2</sub>)(dppe)(η<sup>5</sup>-C<sub>5</sub>H<sub>5</sub>) and **1**, respectively, which involves an excitation from an orbital of Ru d + π C<sub>2</sub> character to a π\* orbital localized on the C<sub>2</sub>C<sub>6</sub>H<sub>4</sub>NO<sub>2</sub> unit. While the β<sub>tot</sub> values for the unsubstituted complexes **2** and Ru(C≡CPh)(dppe)(η<sup>5</sup>-C<sub>5</sub>H<sub>5</sub>) are significantly smaller, due to the absence of a strong donor–acceptor pathway, a similar trend is observed in the calculated β tensors in that β<sub>xxx</sub>, β<sub>xyy</sub> and β<sub>xzz</sub> are major contributors to β<sub>tot</sub>.

#### 4. Conclusion

The present studies have explored the dppf analogues of previously reported dppe-containing complexes as possible NLO materials. Complexes **1** and **2** show comparable or greater quadratic NLO merit than the dppe examples, but with additional redox-switching possibilities due to the presence in **1** and **2** of the electro-active ferrocene-containing diphosphine. Both the linear optical and quadratic NLO observations for **1** and **2** have been rationalized by TD-DFT studies, comparison also being drawn with their dppe-containing cousins. The utility of dppf and other ferrocene-containing species as redox-active auxiliary ligands facilitating the switching of NLO properties is the subject of ongoing studies, and will be reported shortly.

#### Acknowledgements

We thank the Australian Research Council, the Fund for Scientific Research–Flanders (FWO–Vlaanderen; FWO G.0312.08), and the Katholieke Universiteit Leuven (GOA/2011/03) for support of this

work. M.G.H. is an ARC Australian Professorial Fellow, M.P.C. is an ARC Australian Research Fellow, and I.A. was a Postdoctoral Fellow of FWO–Vlaanderen.

#### Appendix A. Supplementary material

CCDC 899522 (**1**) and CCDC 899523 (**2**) contain the supplementary crystallographic data for this paper. These data can be obtained free of charge from The Cambridge Crystallographic Data Centre via [www.ccdc.cam.ac.uk/data\\_request/cif](http://www.ccdc.cam.ac.uk/data_request/cif).

#### References

- [1] N.J. Long, *Angew. Chem., Int. Ed. Engl.* 34 (1995) 21.
- [2] T. Verbiest, S. Houbrechts, M. Kauranen, K. Clays, A. Persoons, *J. Mater. Chem.* 7 (1997) 2175.
- [3] J. Heck, S. Dabek, T. Meyer-Friedrichsen, H. Wong, *Coord. Chem. Rev.* 190–192 (1999) 1217.
- [4] J.P. Morrall, G.T. Dalton, M.G. Humphrey, M. Samoc, *Adv. Organomet. Chem.* 55 (2007) 61.
- [5] M.L.H. Green, S.R. Marder, M.E. Thompson, J.A. Bandy, D. Bloor, P.V. Kolinsky, R.J. Jones, *Nature* 330 (1987) 360.
- [6] T.B. Marder, G. Lesley, Z. Yuan, H.B. Fyfe, P. Chow, G. Stringer, I.R. Jobe, N.J. Taylor, I.D. Williams, S.K. Kurtz, in: S.R. Marder (Ed.), *Materials for Non-linear Optics, Chemical Perspectives*, ACS, Washington D.C., 1991, p. 605.
- [7] P. Nguyen, G. Lesley, T.B. Marder, I. Ledoux, J. Zyss, *Chem. Mater.* 9 (1997) 406.
- [8] C.E. Powell, M.G. Humphrey, *Coord. Chem. Rev.* 248 (2004) 725.
- [9] A.M. McDonagh, I.R. Whittall, M.G. Humphrey, D.C.R. Hockless, B.W. Skelton, A.H. White, *J. Organomet. Chem.* 523 (1996) 33.
- [10] A.M. McDonagh, M.P. Cifuentes, I.R. Whittall, M.G. Humphrey, M. Samoc, B. Luther-Davies, D.C.R. Hockless, *J. Organomet. Chem.* 526 (1996) 99.
- [11] R.H. Naulty, A.M. McDonagh, I.R. Whittall, M.P. Cifuentes, M.G. Humphrey, S. Houbrechts, J. Maes, A. Persoons, G.A. Heath, D.C.R. Hockless, *J. Organomet. Chem.* 563 (1998) 137.
- [12] S.K. Hurst, M.G. Humphrey, J.P. Morrall, M.P. Cifuentes, M. Samoc, B. Luther-Davies, G.A. Heath, A.C. Willis, *J. Organomet. Chem.* 670 (2003) 56.
- [13] K.A. Green, M.P. Cifuentes, M. Samoc, M.G. Humphrey, *Coord. Chem. Rev.* 255 (2011) 2025.
- [14] K.A. Green, M.P. Cifuentes, M. Samoc, M.G. Humphrey, *Coord. Chem. Rev.* 255 (2011) 2530.
- [15] I.R. Whittall, M.G. Humphrey, D.C.R. Hockless, B.W. Skelton, A.H. White, *Organometallics* 14 (1995) 3970.
- [16] I.R. Whittall, M.G. Humphrey, A. Persoons, S. Houbrechts, *Organometallics* 15 (1996) 1935.
- [17] I.R. Whittall, M.G. Humphrey, M. Samoc, J. Swiatkiewicz, B. Luther-Davies, *Organometallics* 14 (1995) 5493.
- [18] I.R. Whittall, M.P. Cifuentes, M.G. Humphrey, B. Luther-Davies, M. Samoc, S. Houbrechts, A. Persoons, G.A. Heath, D.C.R. Hockless, *J. Organomet. Chem.* 549 (1997) 127.
- [19] C.E. Powell, M.P. Cifuentes, A.M. McDonagh, S. Hurst, N.T. Lucas, C.D. Delfs, R. Stranger, M.G. Humphrey, S. Houbrechts, I. Asselberghs, A. Persoons, D.C.R. Hockless, *Inorg. Chim. Acta* 352 (2003) 9.
- [20] M.I. Bruce, I.R. Butler, W.R. Cullen, G.A. Koutsantonis, M.R. Snow, E.R.T. Tiekink, *Aust. J. Chem.* 41 (1988) 963.
- [21] S. Takahashi, Y. Kuroyama, K. Sonogashira, N. Hagihara, *Synthesis* (1980) 627.
- [22] M. Sato, M. Sekino, *J. Organomet. Chem.* 444 (1993) 185.
- [23] Z. Otwinowski, W. Minor, *Methods Enzymol.* 276 (1997) 307.
- [24] R.H. Blessing, *Acta Crystallogr., Sect. A* 51 (1995) 33.
- [25] G.M. Sheldrick, *Acta Crystallogr., Sect. A* 64 (2008) 112.
- [26] O.V. Dolomanov, L.J. Bourhis, R.J. Gildea, J.A.K. Howard, H. Puschmann, *J. Appl. Crystallogr.* 42 (2009) 339.
- [27] P.v.d. Sluis, A.L. Spek, *Acta Crystallogr., Sect. A* 46 (1990) 194.
- [28] K. Clays, A. Persoons, *Phys. Rev. Lett.* 66 (1991) 2980.
- [29] K. Clays, A. Persoons, *Rev. Sci. Instrum.* 63 (1992) 3285.
- [30] E.J. Baerends, T. Ziegler, J. Autschbach, D. Bashford, A. Bérces, F.M. Bickelhaupt, C. Bo, P.M. Boerrigter, L. Cavallo, D.P. Chong, L. Deng, R.M. Dickson, D.E. Ellis, M. van Faassen, L. Fan, T.H. Fischer, C. Fonseca Guerra, A. Ghysels, A. Giammona, S.J.A. van Gisbergen, A.W. Götz, J.A. Groeneveld, O.V. Gritsenko, M. Grüning,

- S. Gusarov, F.E. Harris, P. van den Hoek, C.R. Jacob, H. Jacobsen, L. Jensen, J.W. Kaminski, G. van Kessel, F. Kootstra, A. Kovalenko, M.V. Krykunov, E. van Lenthe, D.A. McCormack, A. Michalak, M. Mitoraj, J. Neugebauer, V.P. Nicu, L. Noodleman, V.P. Osinga, S. Patchkovskii, P.H.T. Philipsen, D. Post, C.C. Pye, W. Ravenek, J.I. Rodríguez, P. Ros, P.R.T. Schipper, G. Schreckenbach, J.S. Seldenthuis, M. Seth, J.G. Snijders, M. Solà, M. Swart, D. Swerhone, G. te Velde, P. Vernooijs, L. Versluis, L. Visscher, O. Visser, F. Wang, T.A. Wesolowski, E.M. van Wezenbeek, G. Wiesnekker, S.K. Wolff, T.K. Woo, A.L. Yakovlev, ADF2012, SCM, Theoretical Chemistry, Vrije Universiteit, Amsterdam, The Netherlands, 2012. <http://www.scm.com>.
- [31] E. van Lenthe, A.E. Ehlers, E.J. Baerends, J. Chem. Phys. 110 (1999) 8943.
- [32] A.D. Becke, Phys. Rev. A 38 (1988) 3098.
- [33] J.P. Perdew, Phys. Rev. B 33 (1986) 8822.
- [34] J.P. Perdew, Phys. Rev. B 34 (1986) 7406.
- [35] O.V. Gritsenko, P.R.T. Schipper, E.J. Baerends, Chem. Phys. Lett. 302 (1999) 199.
- [36] L. Boubekeur-Lecaque, B.J. Coe, K. Clays, S. Foerier, T. Verbiest, I. Asselberghs, J. Am. Chem. Soc. 130 (2008) 3286.
- [37] L. Boubekeur-Lecaque, B.J. Coe, J.A. Harris, M. Helliwell, I. Asselberghs, K. Clays, S. Foerier, T. Verbiest, Inorg. Chem. 50 (2011) 12886.
- [38] S.K. Hurst, M.P. Cifuentes, J.P.L. Morrall, N.T. Lucas, I.R. Whittall, M.G. Humphrey, I. Asselberghs, A. Persoons, M. Samoc, B. Luther-Davies, A.C. Willis, Organometallics 20 (2001) 4664.
- [39] D.A. Kleinman, Phys. Rev. 126 (1962) 1977.